Available online at www.sciencedirect.com
SCIENCE DIRECT
Polymer 46 (2005) 12279–12286
polymer
www.elsevier.com/locate/polymer

Rheological characterization of polydimethylsiloxane/$HTiNbO_5$ nanocomposites prepared by different routes

Alexandre Beigbeder [a], Stéphane Bruzaud [a,*], Pascal Médéric [b], Thierry Aubry [b], Yves Grohens [a]

[a] *Laboratoire Polymères, Propriétés aux Interfaces et Composites, Centre de Recherche, Université de Bretagne Sud, Rue St Maudé, 56321 Lorient cedex, France*
[b] *Laboratoire de Rhéologie, Université de Bretagne Occidentale, 6, Avenue le Gorgeu, C.S. 93837, 29238 Brest cedex 3, France*

Received 22 October 2004; received in revised form 6 October 2005; accepted 17 October 2005
Available online 10 November 2005

Abstract

Polydimethylsiloxane/$HTiNbO_5$ nanocomposites were prepared through four different routes: melt intercalation of the pure mineral, melt intercalation of the organically modified mineral, grafting by a sol–gel process, and grafting by anionic ring-opening polymerization. The four nanocomposites were characterized using wide-angle X-ray scattering and rheometry, at different solid fractions. No exfoliated structure was observed, for any system prepared, but in situ polymerization techniques, especially the ionic polymerization process, were shown to lead to the more structured nanocomposites. This study mainly shows that PDMS master batch made of in situ synthesized systems is probably a well-suited route to achieve high performance silicon elastomer nanocomposites.

Keywords: Polydimethylsiloxane/$HTiNbO_5$ nanocomposites; Rheology; In situ polymerization

1. Introduction

During this last decade, much attention has been paid to polymer nanocomposites especially polymer-layered silicate nanocomposites, which represent a rational alternative to conventional filled polymers. The most often used nanofillers are modified layered clays such as montmorillonite (MMT), bentonite,… [1–6]. Because of their nanometric size and their large active surface, it can be expected that polymeric nanocomposites exhibit improved mechanical, thermal, dimensional and barrier properties compared to pure polymers [1–4]. Nanocomposites are currently prepared through four ways: in situ intercalative polymerization, intercalation of the polymer from a solution, direct intercalation of the molten polymer and sol–gel technology. Whatever the strategy used, it results in the formation of either intercalated or delaminated structure. For the 'intercalated' nanocomposites, a single (and sometimes more than one) extended polymer chain is intercalated between the layers, resulting in a well-ordered multilayer morphology built up with alternating polymeric and inorganic layers. For the 'exfoliated' nanocomposites, the layers are completely delaminated and uniformly dispersed in a continuous polymer matrix.

Melt intercalation is the most common method for the synthesis of nanocomposites. It consists in mixing the polymer and the nanoparticles above the softening point of the polymer.

Synthesis of nanocomposites through in situ intercalative polymerization typically involves intercalation of a suitable monomer followed by polymerization. Polymerization is initiated either by heat or radiation, by the diffusion of an initiator or by an organic initiator or catalyst fixed through cationic exchange inside the interlayer before the swelling step. Various monomers can be used to promote delamination, yielding linear and cross-linked polymer matrixes [4,5].

The sol–gel process, which is mainly based on inorganic polymerization reactions, is a chemical synthesis method initially used for the preparation of inorganic materials such as glasses or ceramics. A large number of polymer–inorganic nanocomposites have been successfully synthesized by performing sol–gel condensation [6]. The advantages of the sol–gel route are a direct and easier dispersion of mineral nanolayers into the liquid precursor at room temperature and the possibility of using a conventional polymer processing technology. This technique has the potential of promoting high dispersion of the mineral nanolayers in a one-step process, without requirement of the presence of ammonium ions.

In the case of polysiloxane nanocomposites, the usual preparation technique is the melt intercalation. First

* Corresponding author. Tel.: +33 2 97 87 45 84; fax: +33 2 97 87 45 88.
E-mail address: stephane.bruzaud@univ-ubs.fr (S. Bruzaud).

0032-3861/$ - see front matter © 2005 Elsevier Ltd. All rights reserved.
doi:10.1016/j.polymer.2005.10.086

Table 1
Composition of the different systems

System	Mineral	Monomer/polymer	Process
1	$HTiNbO_5$	PDMS	Melt intercalation
2	$(Me_4N)_xH_{1-x}TiNbO_5$[a]	PDMS	Melt intercalation
3-1 and 3-2	$HTiNbO_5$ and $(Me_4N)_xH_{1-x}TiNbO_5$[a]	3-Aminopropyldiethoxymethylsilane	Sol–gel route
4	$(Me_4N)_xH_{1-x}TiNbO_5$[a]	D_3	ROP[b]

[a] $x \sim 0.4$.
[b] Ring-opening polymerization.

silanol-terminated polydimethylsiloxane (PDMS) is melt blended with different exchanged MMT, then the silanol end groups are cross-linked. Following this route, exfoliated structure and intercalated structure were both obtained [7].

In this work, we used synthetic mineral oxide $HTiNbO_5$, that was preferred to layered silicates because of its perfect lamellar structure and for its well-defined chemical structure, contrary to layered silicate clays [8]. Furthermore, several studies have demonstrated the possibility of intercalation of voluminous organic molecules inside $HTiNbO_5$ galleries [9,10].

Rheometry is a powerful indirect structural investigation technique, insofar as it is highly sensitive to the state of dispersion and the nature of particle/polymer and particle/particle interactions. Moreover studying rheological properties of such systems is fundamental to improve the processability of these materials, which is of primary importance for their industrial development.

Many works have been published recently on the rheological behaviour of nanocomposites, mainly prepared by melt intercalation. The study of the linear oscillatory shear response, usually expressed in terms of the storage and loss viscoelastic moduli, G' and G'', has attracted particular attention because of its close relation to the mesostructural state of the composite. Indeed the linear dynamic oscillatory shear properties of intercalated and exfoliated nanocomposites in the melt state have been studied for a wide range of polymers [11–14].

The linear viscoelastic response of nanocomposites at low frequencies usually shows a transition from liquid-like to solid-like behaviour for nanocomposites at relatively low silicate loadings (1–2 vol%), with relatively small differences between intercalated and exfoliated systems. This behaviour is often ascribed to the formation, in a quiescent state, of a percolated network [12,14–17].

In this work we used four different routes to achieve polysiloxane-based nanocomposites. Two nanocomposites were prepared by melt intercalation, with and without previous chemical treatment of the mineral oxide; the two other ones by in situ polymerization, namely by anionic polymerization and by a sol–gel process. We characterized the four nanocomposite types focusing on the effect of nanofiller content on their linear viscoelastic properties, determined from oscillatory simple shear measurements. The effect of the preparation route on the clay dispersion state was discussed in the light of the rheological and wide angle X-ray scattering (WAXS) results.

2. Experimental section

2.1. Products

Titanium oxide (Alfa), niobium oxide (ABCR) and potassium carbonate (Merck) were used to synthesize $HTiNbO_5$. Hexamethylcyclotrisiloxane (D_3), tetramethylammonium hydroxide and methyliodide were purchased from Acros, diethoxydimethylsilane and 3-aminopropyldiethoxymethylsilane from ABCR. The linear polydimethylsiloxane ($\bar{M}_n = 10,000$ g mol^{-1}, polydispersity index = 2.4) was supplied by Aldrich.

The $HTiNbO_5$ ($M = 221.8$ g mol^{-1}; $d = 3.55$ g cm^{-3}) oxide was obtained from $KTiNbO_5$ and synthesized as previously described [18]. The resulting product is a white powder that can be easily dispersed in water or alcoholic solvent. The specific surface of the pristine powder, measured by BET, is 0.39 m^2 g^{-1} and the cation exchange capacity (CEC) is (14.5 ± 5) mequiv/100 g prior to any treatment and reaches 1.8 m^2 g^{-1} and (450 ± 5) mequiv/100 g, respectively, after intercalation of tetramethylammonium ions. The aspect ratio of the individual lamellae is estimated to be roughly 500 according to a recent study [19].

2.2. Preparation of nanocomposites

Different polysiloxane/$TiNbO_5$ nanocomposites were prepared at four weight solid fractions, 2, 5, 7 and 10 wt%, following several routes (Table 1).

2.2.1. Melt intercalation: mechanical blending of the mineral and PDMS (system 1)

$HTiNbO_5$ and PDMS matrix were mixed using the Minilab Micro Rheology Compounder (ThermoHaake). The rotational speed, the temperature and the mixing time were fixed at 100 rpm, 25 °C and 10 min, respectively. The preparation route is schematically shown in Fig. 1.

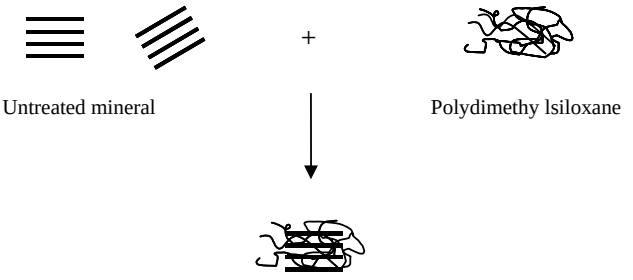

Fig. 1. Schematic illustration of the mechanical blending of the mineral and PDMS.

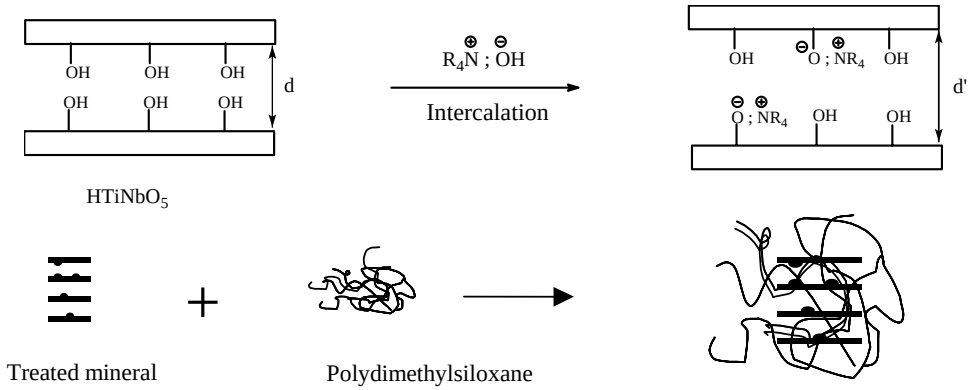

Fig. 2. Schematic illustration of the mechanical blending of the treated mineral and PDMS.

2.2.2. Melt intercalation: mechanical blending of the treated mineral and PDMS (system 2)

An organically modified layered mineral is produced by dispersing $HTiNbO_5$ in water and then treated with a quaternary ammonium hydroxide solution, as shown in Fig. 2. Exchange reaction efficiency is easily estimated by measuring the sample mass increase. The substitution of hydrogen atoms by tetramethylammonium groups leads to a large mass increase, which allows calculating the intercalation percentage x. The treatment results in:

- An almost doubling of the interlayer distance (8.3 – 15 Å), as calculated from the d_{002} diffraction peak in Fig. 5(a) and (b).
- An increase of the organophilic character of the mineral surface [18].

The blending conditions of the treated mineral and the PDMS are the same as those used for system 1.

2.2.3. Grafting by sol–gel process from 3-aminopropyl-diethoxymethylsilane (systems 3-1 and 3-2)

3-Aminopropyldiethoxymethylsilane can be grafted onto $TiNbO_5$ by direct reaction without using any solvent. 3-Aminopropyldiethoxymethylsilane and the mineral were introduced in the reactor under stirring at room temperature during 48 h, as shown in Fig. 3. Few percents of hydrochloric acid (12 mol L^{-1}) were added to the mixture as reaction catalyst. The resulting product was washed three times with toluene and dried under vacuum at 50 °C during one night.

In the first case (system 3-1, starting from non-intercalated $HTiNbO_5$), the polymerization can be achieved through a one-pot process. After a non-optimized polymerization period of

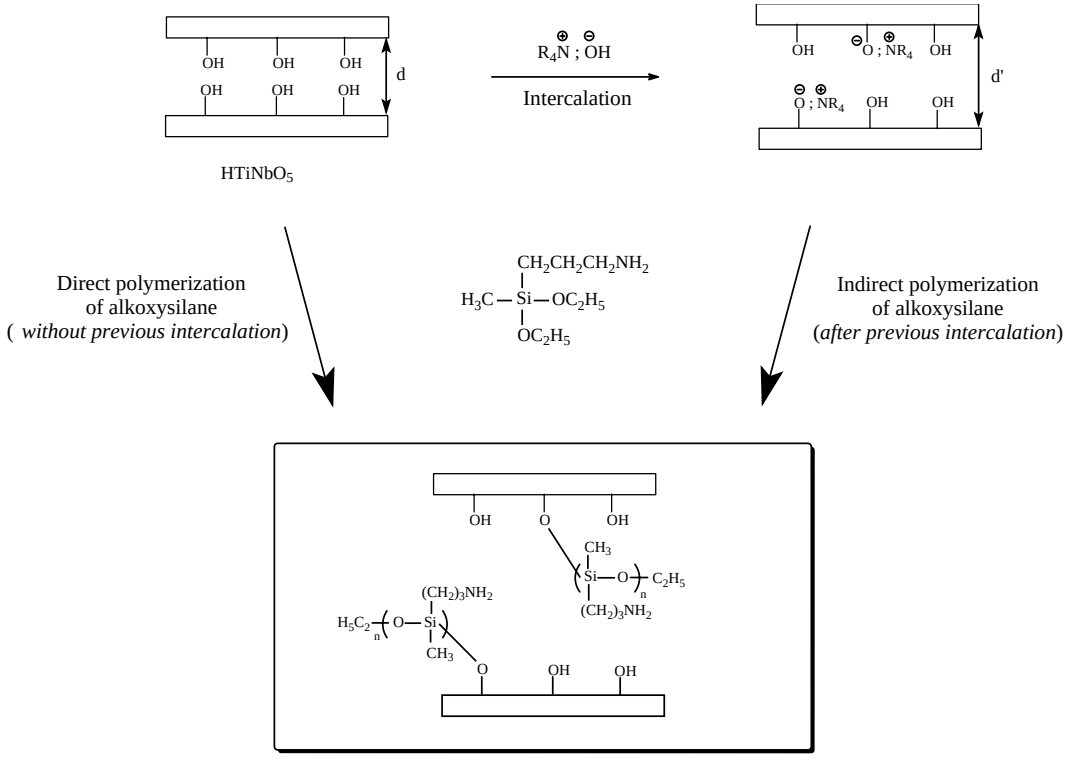

Fig. 3. Schematic illustration of the grafting poly(3-aminopropylmethylsiloxane) onto $HTiNbO_5$ layers.

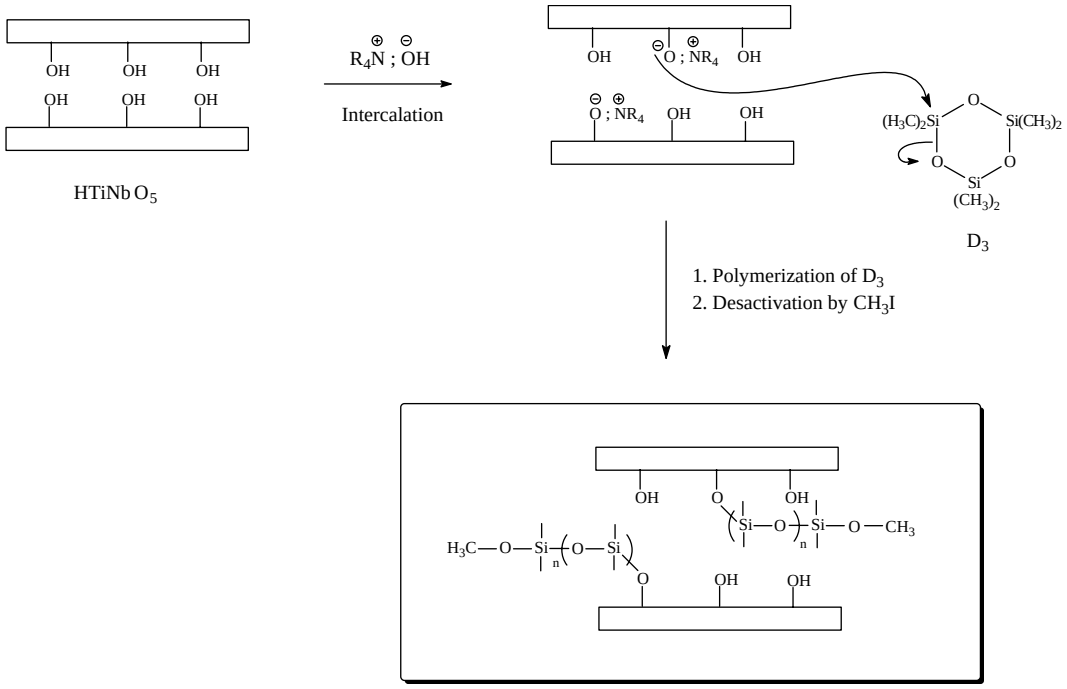

Fig. 4. Schematic illustration of the grafting of PDMS onto $HTiNbO_5$ layers through anionic ring-opening polymerization of hexamethylcylotrisiloxane (D_3).

48 h, the reaction was quenched. Using this polymerization technique allows working at room temperature and needs no solvent and no sonication. We can suppose that the polarity of amino group in 3-aminopropyldiethoxymethylsilane promotes the insertion of the aminoalkoxysilane monomer into the interlayer space.

In the second one (system 3-2, starting from $(Me_4N)_xH_{1-x}TiNbO_5$, $x \sim 0.4$), siloxane chains can be easily grafted to $TiNbO_5$ layers due to an expected larger interlayer space and stronger organophilic character of $(Me_4N)_xH_{1-x}TiNbO_5$ compared to $HTiNbO_5$.

2.2.4. Grafting by anionic ring-opening polymerization of D_3 (system 4)

The preparation of nanocomposites, via in situ intercalative polymerization of cyclosiloxanes in the presence of reactive organophilic $(Me_4N)_xH_{1-x}TiNbO_5$ ($x \sim 0.4$), and their characterization were described in a previous paper [18]. The originality of the process lies in the choice of the polymerization method to graft polysiloxane to $TiNbO_5$ layers through an acid–base reaction between $HTiNbO_5$ and tetramethylammonium hydroxide, as shown in Fig. 4.

Nanocomposites were synthesized by emulsion polymerization of hexamethylcyclotrisiloxane (D_3) from organophilic $(Me_4N)_xH_{1-x}TiNbO_5$ previously prepared. Anionic ring-opening polymerization was initiated by the mineral-supported oxygen anions associated to the Me_4N^+ counter-ions acting as a phase transfer catalyst. At the end of the reaction, the resulting product was treated with excess methyl iodide (Fig. 4). The sonication time and the reaction temperature were fixed at 3 h and 50 °C, respectively. The reaction is achieved in about 70 h. Finally, the resulting compound must be washed several times with toluene to eliminate possibly ungrafted polymers and residual monomers from the nanocomposite. Experimental results show an important increase of sample weight, attributed to the formation of polydimethylsiloxane/$TiNbO_5$ composites, prepared in aqueous medium according to this original process (Table 2) [20]. The efficiency of grafting reactions was studied using ^{29}Si CP-MAS NMR [21]. The spectrum presents a specific signal ascribed to PDMS chain chemical grafting onto the $HTiNbO_5$ surface.

2.3. Rheological characterization

The linear viscoelastic behaviour of the nanocomposites prepared was determined using oscillatory simple shear tests on a controlled stress Carrimed CSL-50 rheometer, equipped with a cone and plate geometry (diameter 6 cm, angle 2°). All measurements were performed at 20 °C. Linear viscoelastic measurements were performed for all samples following two steps. First, a strain sweep experiment was performed at a fixed frequency of 1 Hz, in order to determine the extent of the linear

Table 2
Experimental results for the preparation of nanocomposites (system 4)

$(Me_4N)_xH_{1-x}TiNbO_5$[a] initial mass (g)	Nanocomposite final mass (g)	Mass increase (%)
0.597	1.208	102
0.503	1.550	208

[a] $x \sim 0.4$.

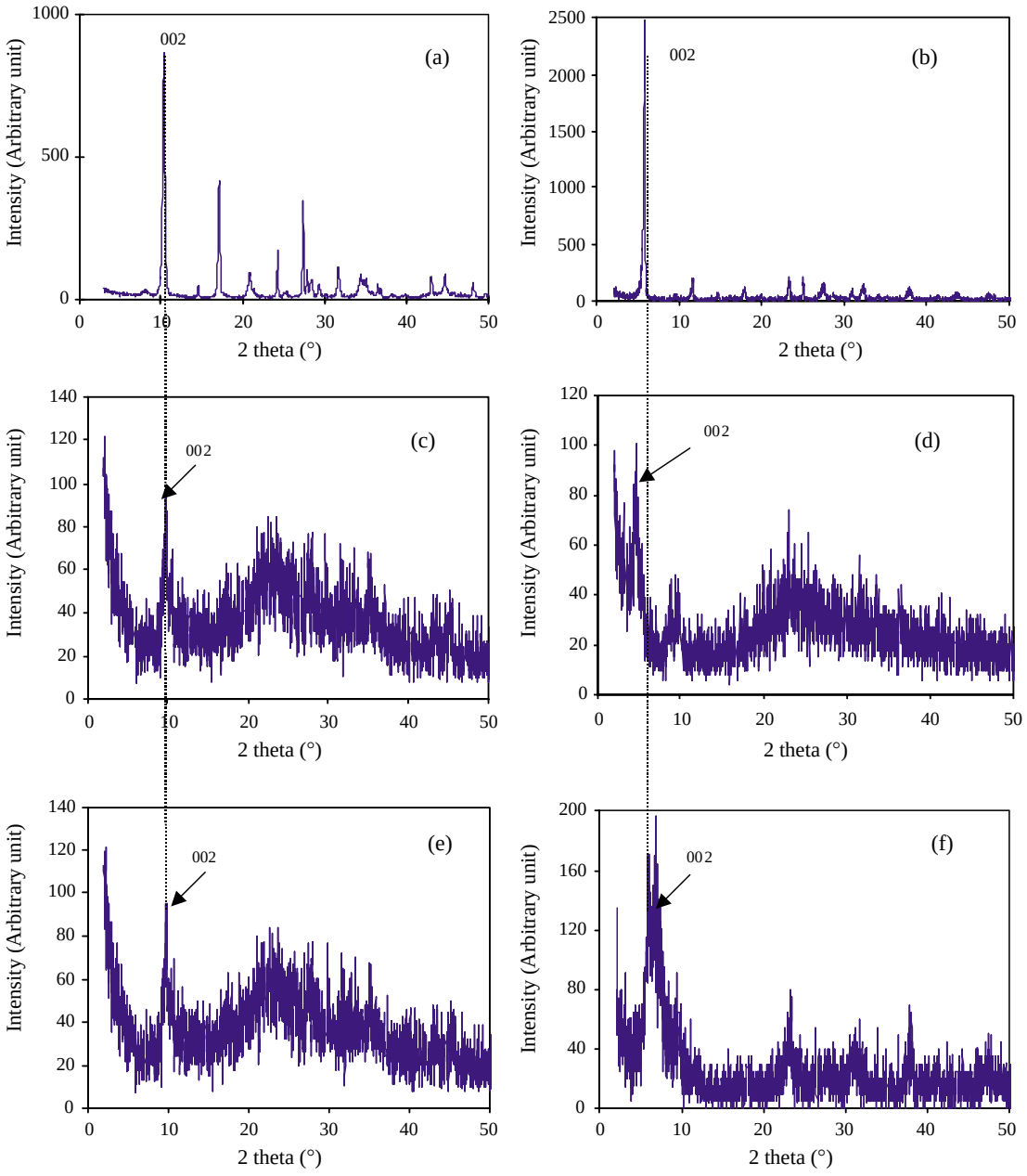

Fig. 5. WAXS diagrams of (a) $HTiNbO_5$; (b) $(Me_4N)_xH_{1-x}TiNbO_5$; (c) system 1; (d) system 2; (e) system 3 and (f) system 4.

viscoelastic regime of the samples; second, a frequency sweep experiment, over a frequency range from 0.1 to 10 Hz, performed at a fixed strain chosen in the higher frequency region of the linear viscoelastic domain, in order to characterize the viscoelastic response on different time-scales. The amplitude of the imposed strain was 10% for systems 1 and 2, 1% for systems 3 and 0.5% for system 4.

2.4. Wide angle X-ray scattering characterization

Wide angle X-ray scattering (WAXS) data were collected using a Philips PW3710 diffractometer equipped with the goniometric X'PERT system. The instrument uses radiation from a copper target tube (Cu Kα radiation; $\lambda = 1.54$ Å).

$HTiNbO_5$, $(Me_4N)_xH_{1-x}TiNbO_5$, systems 1, 2, 3 and 4 were characterized by WAXS (Fig. 5).

3. Results

The linear viscoelastic behaviour of the PDMS matrix is shown in Fig. 6. The curves exhibit two main features:

– An extended linear viscoelastic domain, up to several hundreds percent.

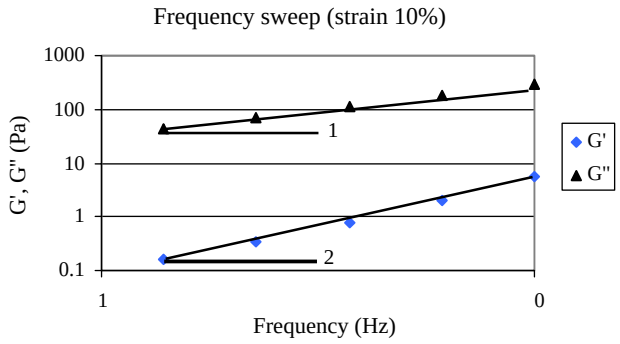

Fig. 6. Viscoelastic moduli, G' and G'', as a function of frequency, for PDMS matrix.

– The existence of a terminal regime, characterized by a quadratic frequency dependence of the storage modulus, and a linear frequency dependence of the loss modulus, in the range 1 – 10 Hz.

3.1. System 1

The storage modulus, G' of system 1 is plotted in Fig. 7 as a function of frequency. Fig. 7 shows that:

– No G' plateau was observed whatever the amount of fillers incorporated.
– A very slight increase of the G' values was observed as the mineral content was increased. However, these values remained very low, indeed they did not exceed 0.1 Pa at a solid fraction of 10 wt%.

The loss modulus G'' did not exhibit any significant difference with that of the pure PDMS, and was not plotted for the sake of clarity. Moreover, for all system 1 samples tested $G' \ll G''$; for example, at a frequency of 1 Hz and for a 5 wt% nanocomposite, the ratio G'/G'' was shown to be about 1/100.

WAXS diffraction patterns (Fig. 5(c)) show a low intensity d_{002} diffraction peak, located at the same Bragg angle as that for the pure mineral, meaning that the interlayer distance of the few remaining layered stacks is the same as that measured for pure $HNbTiO_5$ [18].

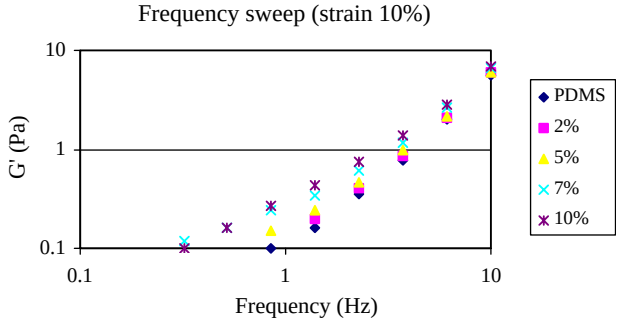

Fig. 7. Storage modulus, G', as a function of frequency, for system 1, at different mass solid fractions.

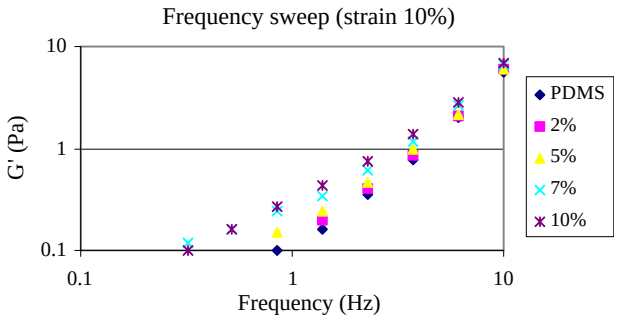

Fig. 8. Storage modulus, G', as a function of frequency, for system 2, at different mass solid fractions.

3.2. System 2

The rheological results for system 2 are plotted in Fig. 8. A slight G' plateau is observed for G' at the lowest frequencies, for the 7 and 10 wt% nanocomposites. This plateau is observed at frequencies lower than 1 Hz. Similar characteristics were observed in the literature for other nanocomposites [13,14].

The increase of G' with mineral loading is more pronounced than for sytem 1, since G' reaches 1 Pa for 10 wt% nanocomposites. Nevertheless, as for system 1, G' is low compared to G' for all system 2 samples tested; for example, at a frequency of 1 Hz and a solid fraction of 5 wt%, the ratio G'/G'' is about 1/100.

The WAXS diffractogram (Fig. 5(d)) shows the presence of few layered stacks characterized by an average interlayer distance of 10 Å, corresponding to the low intensity d_{002} diffraction peak at $2\theta = 4.5°$. This intergallery height is lower than that due to the intercalation of tetramethylammonium ions between mineral layers [18].

3.3. System 3

Since the rheological results for system 3-1 and 3-2 are similar, we only present the results obtained for system 3-1. The results are shown in Fig. 9. The slope of the low frequency region of the G' vs. frequency curves decreases significantly for nanofiller content of 2 and 5 wt%, and a clear plateau is observed for 7 and 10 wt% nanocomposites. Moreover, the G' plateau is observed on a broader frequency range (0.1–10 Hz) than for the previous systems.

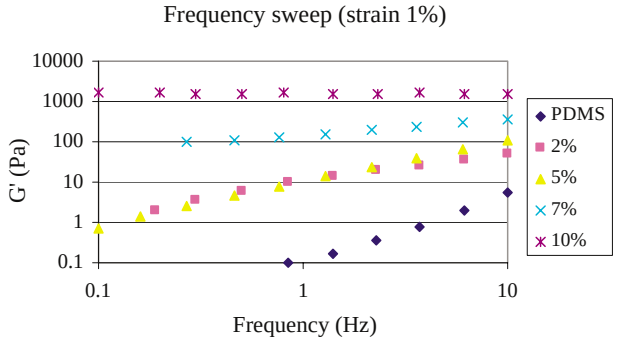

Fig. 9. Storage modulus, G', as a function of frequency, for system 3, at different mass solid fractions.

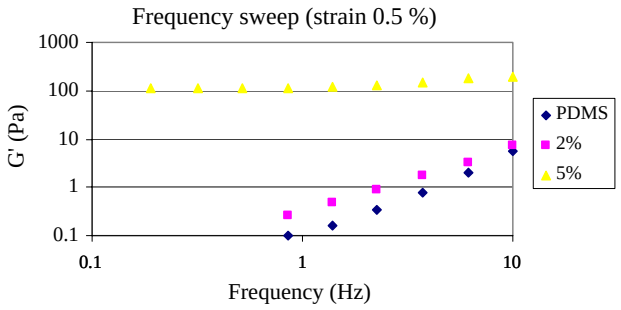

Fig. 10. Storage modulus, G', as a function of frequency, for system 4, at different mass solid fractions.

The increase of G' with mineral loading is larger than for systems 1 and 2; G' reaches a value of 1000 Pa at a mineral content of 10 wt%. G' is still inferior to G'' for all system 3 samples tested; for example the G'/G'' ratio, at a frequency of 1 Hz and at a solid fraction of 5 wt%, is about 1/10.

WAXS pattern of system 3 (Fig. 5(c)) is similar to that of system 1; it exhibits a low intensity d_{002} diffraction peak, located at the same Bragg's angle as that for the pure mineral, meaning that the interlayer distance of the few remaining layered stacks is the same as that measured for pure $HNbTiO_5$.

3.4. System 4

The storage modulus, G', as a function of frequency is plotted in Fig. 10. A clear G' plateau is observed at 5 wt% filler content, whereas no effect is seen for the 2 wt% nanocomposites. This plateau extends over the same frequency range (0.1–10 Hz) as that observed for system 3. The G' value strongly increases between 2 wt% solid fraction, for which the behaviour is close to the PDMS matrix, and 5 wt% solid fraction, for which a value of 100 Pa is reached. Moreover, the ratio G'/G'' is 3/2 at a frequency of 1 Hz and for a 5 wt% nanocomposite, that is much larger than for any other systems studied.

For this system, the WAXS diffractogram (Fig. 5(f)) shows the presence of few layered stacks characterized by an average interlayer distance of 15 Å, corresponding to the diffraction peak at $2\theta = 6.5°$. This intergallery height corresponds to the intercalation of tetramethylammonium ions between mineral layers [18].

4. Concluding discussion

First of all, we would like to point out that wide-angle X-ray scattering does not seem to be a reliable investigation technique in order to compare the different nanocomposites studied in this work. Indeed, the X-ray diffraction patterns are difficult to interpret and correlate with the rheological behaviors. All diffractograms exhibit a low intensity d_{002} diffraction peak, at a Bragg's angle equal to that of the pure or organically modified mineral, used for preparation. As expected, pretreating the mineral leads to an increase, a nearly doubling, of the interlayer space. The fact that such intergallery heights can be measured means that layered stacks are present in all samples tested, showing that exfoliation was not completely achieved in any nanocomposites prepared. Nevertheless, the intensity of the diffraction peaks being low, the layered mineral stacks are expected to be few within the samples. Therefore, the structure of all nanocomposites prepared in this study can be mostly described as partially exfoliated, but differences in precise structural organization cannot be assessed using WAXS data.

On the contrary, rheological results clearly show significant differences between the four types of nanocomposites, which allows to draw up a hierarchy of these systems, according to their preparation route. Starting from the 'less good' up to the 'best' system:

(1) For system 1, the addition of mineral yields rheological effects expected for classical fillers, such as those observed for micron scale aggregates of TiO_2 or $CaCO_3$ in molten polymer matrix, for instance; this system can, therefore, be seen as a microcomposite. This conclusion is not surprising, in so far as the mineral has no particular affinity toward the matrix in system 1.
(2) In system 2, the intercalation of tetramethylammonium ions inside the mineral galleries, before mechanical mixing with PDMS, leads to an increase of the cohesive and elastic properties of the nanocomposites at relatively low volume fractions and over a limited frequency range, even though the dissipative part of the viscoelastic response is still predominant. Despite preliminary chemical treatment with tetramethylammonium ions, system 2 can, therefore, be seen as a weakly structured nanocomposite.
(3) In system 3, the in situ polycondensation of alkoxysilanes seems to be a rather efficient route. Indeed systems 3 exhibits a more marked elastic and cohesive behavior than system 2, at relatively low volume fractions and over a larger frequency range. Furthermore, even though the dissipative part of the viscoelastic response is still predominant, the ratio of the elastic over the dissipative contribution increases.
(4) System 4 is certainly the 'best' nanocomposite prepared in this study, at least it is the most structured one. Indeed its elastic behavior is well marked at low volume fractions and the dissipative contribution to the linear viscoelastic response is less pronounced, even though not negligeable. In other words, among the four nanocomposites prepared, this system is certainly the one in which connectivity is best achieved.

As a conclusion, this work clearly shows that the elaboration methods of nanocomposites have much influence on their structure and rheology. In the case of polydimethylsiloxane/$HTiNbO_5$ nanocomposites, this study shows that:

– No preparation method used leads to an exfoliated structure.
– Melt intercalation requires preliminary intercalation by quaternary ammonium ions.

– A more cohesive structure is obtained when the elaboration path starts from monomers in order to chemically graft polymer chains at the surface of mineral layer (in situ polymerization).
– Anionic polymerization is more efficient than polycondensation in term of nanocomposite structuration.

Finally, it should be pointed out that all PDMS nanocomposites characterized in this work, even the 'best' one (i.e. system 4), are less structured than other layered silicate nanocomposites [13]. This may be one of the reasons why only few articles have been published on PDMS nanocomposites, in spite of its many potential applications. Nevertheless, this work tends to show that PDMS master batch made of in situ synthesized systems is probably a well-suited route to achieve high performance silicon elastomer nanocomposites.

References

[1] Burnside SD, Giannelis EP. Chem Mater 1995;7(9):1597–600.
[2] Giannelis EP, Krishnamoorti R, Manias E. Adv Polym Sci 1999;138: 107–47.
[3] Alexandre M, Dubois P. Mater Sci Eng 2000;R28:1–63.
[4] Strawhecker KE, Manias E. Chem Mater 2000;12(10):2943–9.
[5] Okamoto M, Ray SS. Prog Polym Sci 2003;11:1539–641.
[6] Wen J, Wilkes GL. Chem Mater 1996;8(8):1667–80.
[7] Wang SJ, Long CF, Wang XY, Li Q, Qi ZN. J Appl Polym Sci 1998;69: 1557–61.
[8] Rebbah H, Desgardin G, Raveau B. Mater Res Bull 1979;14:1125–31.
[9] Rebbah H, Borel MM, Raveau B. Mater Res Bull 1980;15:317–21.
[10] Kikkawa S, Koizumi M. Mater Res Bull 1980;15:533–9.
[11] Hyun YH, Lim ST, Choi HJ, Jhon MS. Macromolecules 2001;34(23): 8084–93.
[12] Hoffmann B, Dietrich C, Thomann T, Friedrich C, Mulhaupt R. Macromol Rapid Commun 2000;21(1):57–61.
[13] Solomon MJ, Almusallam AS, Seefeldt KF, Somwangthanaroj A, Varadan P. Macromolecules 2001;34(6):1864–72.
[14] Ren J, Silva A, Krishnamoorti R. Macromolecules 2000;33(10):3739–46.
[15] Larson R. The structure and rheology of complex fluids. Oxford: Oxford University Press; 1999.
[16] Krishnamoorti R, Giannnelis EP. Macromolecules 1997;30(14): 4097–102.
[17] Kim TH, Lim TL, Lee CH, Choi HJ, Jhon MS. J Appl Polym Sci 2003;87: 2106–12.
[18] Bruzaud S, Levesque G. Chem Mater 2002;14(5):2421–6.
[19] Du GH, Yu Y, Chen Q, Wang RH, Zhou W, Peng LM. Chem Phys Lett 2003;377:445–8.
[20] GPC measurements are not possible because all the obtained nanocomposites are insoluble in usual organic solvents. So, only silicon elemental analysis carried out on polysiloxane-*g*-$TiNbO_5$ materials allowed to calculate the silicon containing polymer ratio incorporated in the nanocomposite (Si % up to 18). The average number of siloxane units grafted on mineral layers can be evaluated to 8–10 (relative to each $TiNbO_5$ unit).
[21] Beigbeder A, Bruzaud S, Spevacek J, Brus J, Grohens Y. Macromol Symp 2005;222:225–31.